Spatial-Temporal Trends of Rainfall, Maximum and Minimum Temperatures Over West Africa

Francis Muthoni

***Abstract*—This article investigates the magnitude and significance of spatial-temporal trends of 37 years' time series of the gridded data for rainfall, maximum (Tmax) and minimum (Tmin) temperature for West Africa. A modified Mann-Kendall test and Theil-Sen's slope estimator were utilized to test the significance and the magnitude of trends, respectively. The magnitude of significant trends for three variables between six agroecological zones (AEZs) was compared. Gridded climate data represented gauge data with high accuracy and, therefore, can reliably complement the sparse observation network in West Africa. The three variables showed significant positive and negative trends of varying magnitude and spatial extent. June to September rainfall showed a positive increase (0.1–5 mm/month/year) that mostly occurred north of 11° latitude. October rainfall showed a positive trend across the region, but the magnitude was higher south of the same latitude. A widespread significant warming trend was observed across all AEZs and months. However, a localized cooling in August and September over the Sahel and Sudan Savanna was an exception. The cooling over the two AEZs coincided with a positive trend of rainfall. The zonal analysis revealed that the magnitude of the positive trend of June, September, and October rain increased following a North–South gradient from the Sahel to humid forest AEZs. Results provide spatial evidence of climate change in a limited data environment to guide the targeting of appropriate adaptation measures. The information generated from this article helps the design of early warning systems against droughts and floods.**

***Index Terms*—Agroecological zones (AEZs), climate hazards group infrared precipitation with stations (CHIRPS), CHIRTSmax, satellite time series, spatial-temporal trends, TerraClimate (TC).**

I. Introduction

CLIMATE change and variability have significant positive or negative impacts on the productivity and resilience of agroecosystems across different regions [1]–[3]. These impacts are more severe in predominantly rain-fed agricultural systems in Africa, where they confound with extreme poverty and rapid population growth [4]. The fifth assessment report of the United Nations Intergovernmental Panel on Climate Change (IPCC) estimated increased warming and wet season rainfall over Africa's landmass [5]. Trend analysis using time series of coarse resolution remote sensing data over tropical Africa shows an annual mean temperature increase at a rate of 0.15 °C per decade from 1979 to 2010 [6]. Predictions for rainfall are most uncertain primarily due to limited understanding of tropical rain forming processes.

The magnitude of climate change and variability is heterogeneous over space and time. Mapping spatial-temporal trends of climate variables in Africa is challenging due to a sparse gauge network and declining measurements from the existing stations [7], [8]. The prevalent heterogeneous climatic gradients further complicate the scarcity of the gauge network. The density of gauge stations in Africa is 1 per 26 000 km^2, which is eight times lower than minimum recommendations by the World Meteorological Organization [9]. Gaps in gauge stations measurements in Africa have increased by over 50% since 1900. Climate analysis using data from a few sentinel gauge stations are used to draw conclusions over vast spatial extents. Recent studies have examined climatic trends in West Africa using only gauge station data, for example [10], [11]. However, the information generated from such studies can reliably support agro-advisories for a short radius surrounding the stations, given the inherent heterogeneity in topography, which introduces sharp gradients such as rain-shadow effect. Trends for climatic variables in Africa have been investigated using coarse resolution remote sensing or reanalysis data; for example, Collins [6] analyzed gridded data with 2.5° × 2.5° spatial resolution. Coarse-resolution data mask out important climatic details that can misinform policymaking. Therefore, discerning the spatial distribution of change and variability, especially for rainfall and extremes temperatures, using fine-resolution data is necessary to facilitate better targeting of appropriate adaptive measures.

Improved availability and accuracy of long time series of gridded climate data obtained from remote sensing satellites and reanalysis systems can complement the limitation of a sparse gauge network in Africa. The relatively new open access sources of high resolution gridded climate data sets include the climate hazards group infrared precipitation with stations (CHIRPS-v2 [12], climate hazards center infrared temperature with stations (CHIRTSmax) [13] and TerraClimate surfaces (TC) [14]. However, these new gridded layers need rigorous evaluation against existing ground gauge observations to ascertain their accuracy and inform resource managers on which datasets could be appropriate for specific applications or locations. Several studies have attempted to validate gridded time series data for rainfall in West Africa at the catchment [15] or (sub)-national [16] and regional

Manuscript received October 5, 2019; revised March 31, 2020 and May 2, 2020; accepted May 19, 2020. Date of publication May 25, 2020; date of current version June 16, 2020. This work was supported by USAID under Grant AID-BFS- G-11-00002 under the Feed the Future initiative to support the Africa RISING program – Sustainable Intensification of Key Farming Systems in the Sudano-Sahelian Zone of West Africa.

The author is with the Africa RISING Program, International Institute of Tropical Agriculture, Duluti 200001, Tanzania (e-mail: fkmuthoni@gmail.com).

This article has supplementary downloadable material available at http://ieeexplore.ieee.org, provided by the authors.

Digital Object Identifier 10.1109/JSTARS.2020.2997075

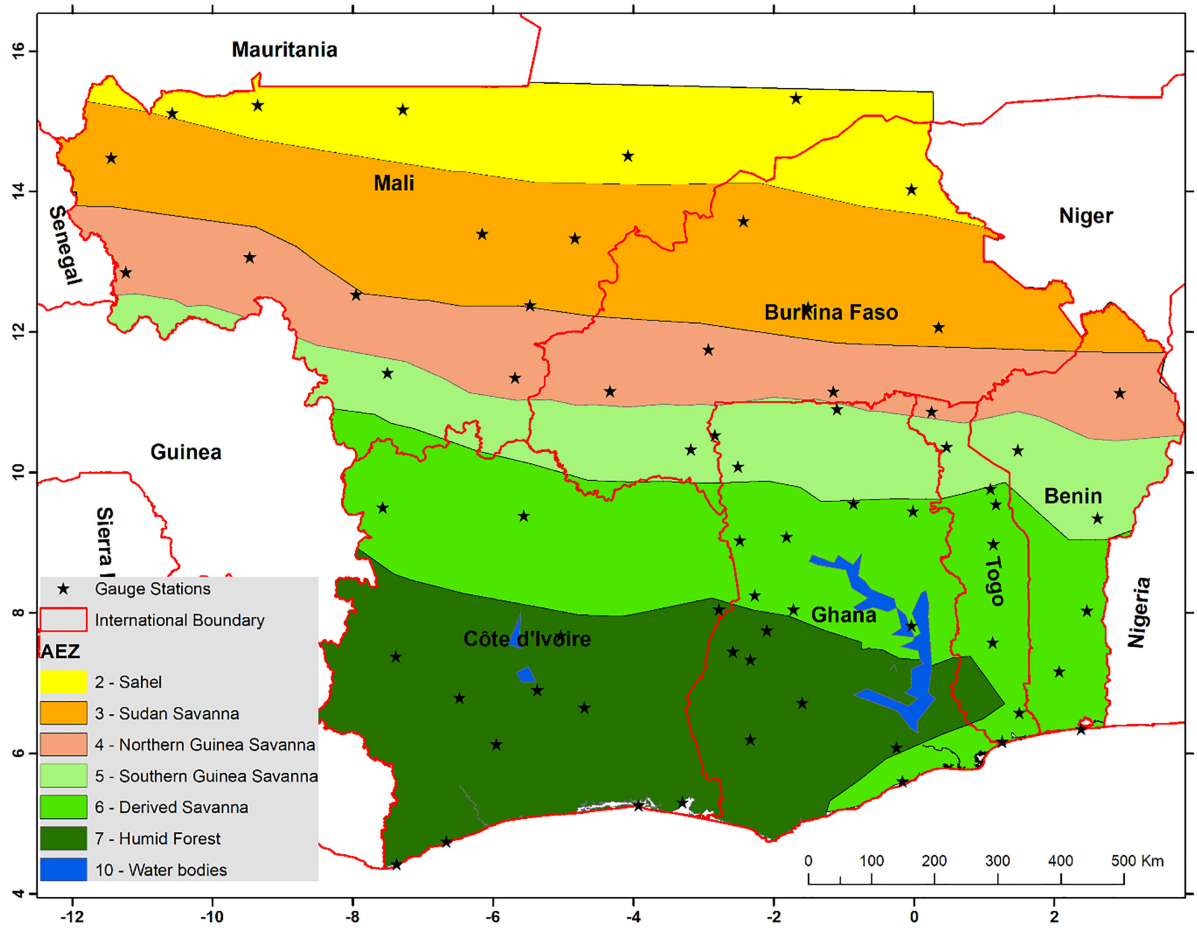

Fig. 1. Location of the study area. The 66 gauge stations used to evaluate the accuracy of gridded climatic data are superimposed on six AEZs over six countries in the West Africa region.

[17] scales. These evaluations revealed significant disparities in the skill of the satellite rainfall estimates. There is no single best product as their accuracy is dependent on rainfall characteristics considered (e.g., amount, intensity, and frequency) [18], the timescale of observation [7], [19], [20], and elevation gradients [21].

There are fewer meteorological stations that record temperature variables, and existing observations are much shorter compared to rainfall [22], [23]. Moreover, there is limited knowledge on spatial-temporal trends of temperature extremes despite heat stress being one of the critical factors limiting agricultural productivity. Furthermore, several studies examined annual trends of climatic variables, hence masking intra-annual dynamics that are important in regulating seasonal calendars. Rainfall, minimum (Tmin) and maximum (Tmax) temperature are the most critical climatic variables that significantly limit crop yields. Monitoring the long-term spatial-temporal trends of the three climatic variables is vital for generating knowledge that would support evidence-based design or scaling out of best-bet climate-smart agriculture strategies. Mapping climatic trends can help to identify areas that agriculture is vulnerable to extreme weather events such as frequent droughts, flooding, and frost.

This article evaluates the accuracy of recently released satellite-based, and reanalysis gridded climatic variables (rainfall, Tmin, and Tmax) obtained from Climate Hazards Group (CHG) and TerraClimate (TC) databases respectively against observations recorded by ground stations at monthly temporal resolution. It further investigates the significance and the magnitude of monthly trends for three climatic variables for the last 37 years (1981–2017) over six countries in West Africa. Moreover, it compares climatic trends over six agroecological zones (AEZs).

II. Material and Methods

A. Study Area

The study area covers approximately 2.2 million km^2 over six countries in the West Africa region. However, it excludes part of Mali territory located in the desert AEZ, where there is minimal agricultural cultivation (see Fig.1). The altitude ranges from 0 to 1300 m above sea level.

Annual rainfall ranges from 200 to 2400 mm and is characterized by high interannual variability. Rains are primarily influenced by the migration of the intertropical discontinuity (ITD) that regulates the West African Monsoon by oscillating

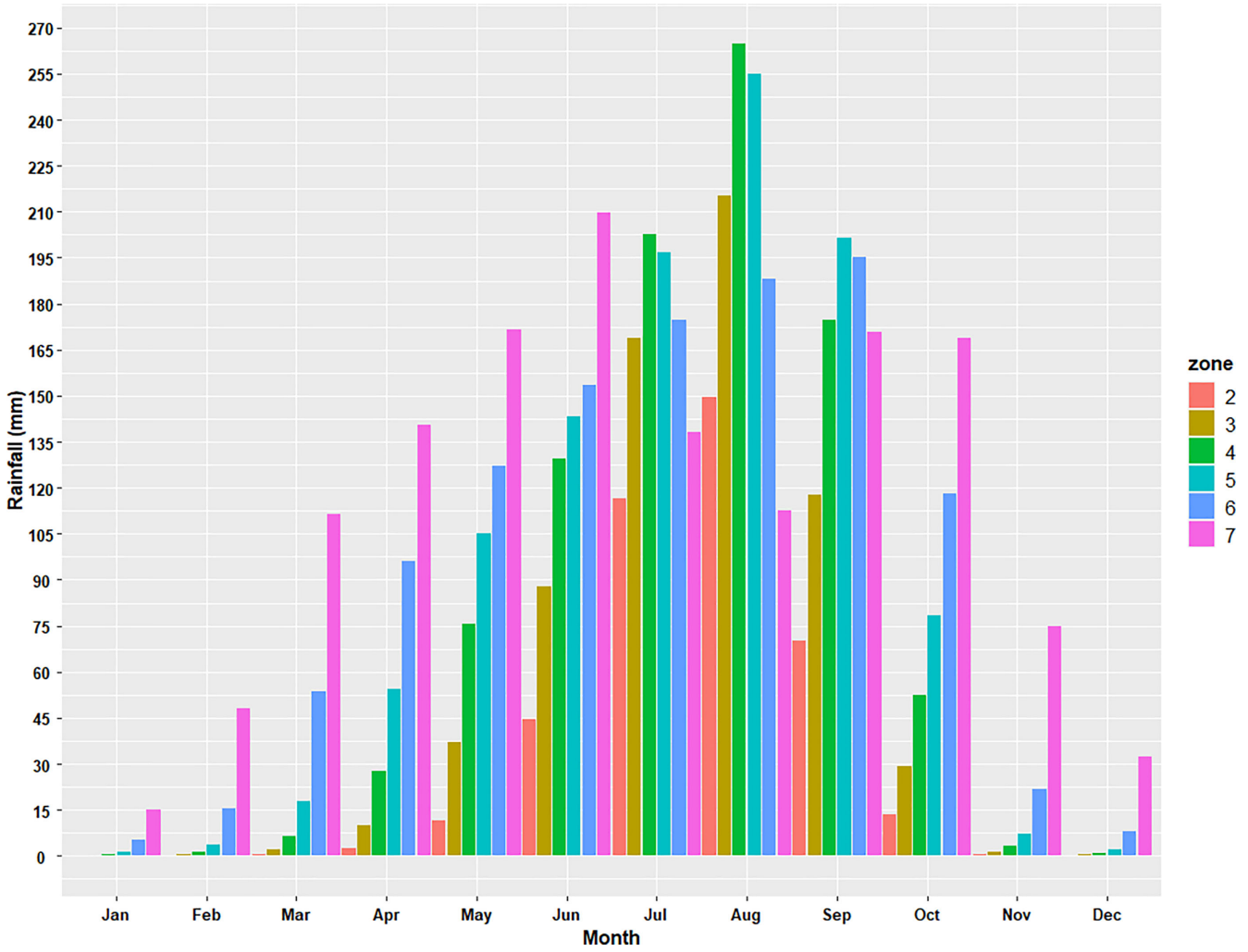

Fig. 2. Climatological cycle of the mean annual rainfall for the six agroclimatic zones over the study region. The codes for AEZs are 2 (Sahel), 3 (Sudan Savanna), 4 (Northern Guinea Savanna), 5 (Southern Guinea Savanna), 6 (Derived Savanna), and 7 (humid forest). Rainfall data obtained from the CHIRPS-v2 database.

south to north and back [24]. Areas located south of the ITD are regulated by moisture-laden south-westerly winds that blow moist air from the Gulf of Guinea onto the hinterland [16]. The region located north of ITD is regulated by north-easterly Harmattan winds that bring dry and dusty winds from the Sahara desert between November and March. The Sahel and the four immediate Savannah agroecologies (see Fig. 1) experience unimodal rainfall between April and October that is regulated by the migration of ITD to its northernmost boundary (see Fig. 2). The humid forest agroecology experience two wet seasons: the major wet season from March to July and the minor wet season from September to November (see Fig. 2).

Agriculture is the main economic activity in the region with diverse crops depending on agroecology. Crops grown in the Sahel and four consequent savannas agroecologies (see Fig. 1) include Pearl millet (*Pennisetum glaucum*), sorghum (*Sorghum bicolor*), maize (*Zea mays*), and lowland rice (*Oryza* spp). Livestock keeping is practiced mainly in a transhumance system, where it is a significant source of livelihood.

B. Climatic Variables

Gridded monthly total rainfall data were obtained from TC [14] and CHIRPS-v2 [12] databases. Gridded monthly mean maximum temperatures (Tmax) data were obtained from TC and CHIRTSmax [13] databases. Gridded monthly mean minimum temperatures (Tmin) were only available from the TC database. The TC database provides monthly climate data with a 4-km spatial resolution covering the global terrestrial surface from 1958 to 2018. The primary weather variables available in the TC database are Tmin, Tmax, total rainfall, vapor pressure, downward surface shortwave radiation, and wind-speed. The TC gridded layers are generated using a climatically aided interpolation that combines high-resolution climatological fields from WorldClim database [25] with coarser resolution temporal anomalies from Climate Research Unit time series data version 4 (CRU Ts4.0) [26] and the Japanese 55-year Reanalysis [27].

CHIRPS-v2 and CHIRTSmax products are produced by the US Geological Survey and the Climate Hazard Group at the

University of California, Santa Barbara. CHIRPS-v2 algorithm blends data from three main sources.

1) The CHG precipitation climatology with 0.05° spatial resolution, which is estimated monthly from station data, average satellite observations, elevation, latitude, and longitude.
2) The CHG thermal infrared-based satellite precipitation estimate (CHIRP).
3) The *in situ* rain gauge measurements [12].

CHIRPS-v2 data are available from 1981 to-date at daily, pentad (5 days), and monthly temporal scales at approximately 5.5-km spatial resolution with quasi-global land coverage (50°S–50°N). Like CHIRPS-v2 data, CHIRTSmax is estimated from three main inputs.

1) A high-resolution 0.05° monthly climatology capturing spatial variability.
2) GeoSat Infrared data that capture the temporal variability.
3) Available ground observations of Tmax [13].

However, the algorithm for CHIRTSmax uses a moving window regression instead of interpolation that is applied to estimate CHIRPS-v2 data. For each month and location, the thermal infrared and the interpolated station components were blended, based on weights derived from an empirical spatial covariogram and the distance to the nearest station. Grid cells near stations favor the interpolated station data, while values far from stations primarily depend on the satellite temperature fields. These blended anomaly fields were added to the Tmax climatology to produce the CHIRTSmax surface. The dataset is available from 1983 to 2016 at ∼5.5-km spatial resolution at the Equator and near-global extent (70°N–60°S).

The accuracy of two different monthly gridded rainfall and Tmax products was compared since the datasets are relatively new. Comparing the accuracy of new products is logical to determine which is accurate at different locations and biophysical conditions. To the best of the author's knowledge, the accuracy of TC and CHIRTSmax products have not been evaluated in the study area. However, recent studies have evaluated the accuracy of CHIRPS-v2 rainfall at different spatial extents over the West Africa region [18], [28]. The monthly temporal scale was selected because the TC grid layers are only available at that interval. Moreover, recent evaluations of gridded rainfall products in the West Africa region revealed that their agreement with gauge observations is significantly better at monthly compared to daily and decadal temporal scales [18], [28]. Assessing climatic trends from annually aggregated data could mask out significant intra- and interannual variations considering that different locations can experience similar total annual rainfall but with a contrasting temporal distribution. Therefore, monthly climatic data better represent the differences in cropping calendar activities at different locations compared to annual trends. Each input grid comprised of a 37 years monthly time series (1981–2017; $n = 444$ layers), except CHIRTSmax that was available between 1983 and 2016. The year 1981 was selected as the start date of analysis based on the availability of most gridded climate layers.

Daily and monthly rainfall, Tmin and Tmax data for 66 ground weather gauge stations (see Fig. 1, Appendix A) were obtained from national meteorological services and the global summary of the month (GSOM) database [29]. The GSOM database contains quality controlled monthly summaries of more than 50 weather variables computed from stations in the Global Historical Climatology Network Daily database [30]. The daily gauge records were aggregated to monthly total rainfall and monthly mean for Tmin and Tmax before merging with the monthly dataset obtained from GSOM.

A map of AEZs with six distinct classes across the study area was used to define climatic zonation (see Fig 1). The AEZ map was produced after modifications of the agro-climatic zonation map produced by [31] after integrating information on the length of the growing season from [32]. These AEZs are here-after referred to zones 2 (Sahel), 3 (Sudan Savanna), 4 (Northern Guinea Savanna), 5 (Southern Guinea Savanna), 6 (Derived Savanna), and 7 (humid forest).

C. Data Analysis

1) Validation of Climatic Variables With Gauge Data: A point to pixel validation approach was used, whereby values of grid cells were extracted and matched with those recorded at colocated gauge stations. The agreement between monthly gridded data and gauge station data was evaluated using a modified Kling–Gupta efficiency (KGE) [33]. The KGE was decomposed into the three individual elements, i.e., Pearson product-moment correlation coefficient (r), bias (β), and variability (γ). The goodness of fit statistics was generated using "HydroGOF" R package [34]. The r measures the linear correlation between the time series of observed gauge data and satellite rainfall estimates (temporal dynamics). The β measures the average tendency of the satellite values to be larger ($\beta > 1$, overestimation) or smaller ($\beta < 1$, underestimation) than gauge data (bias). The γ shows whether the dispersion of satellite estimates is higher or lower compared to gauge observations (variability).

Moreover, the agreement was evaluated using the root-mean-square error (RMSE) that is the standard deviation of the difference between gridded estimates and gauge observations. High RMSE indicates a considerable difference between gridded estimates and gauge measurements and vice versa. Among the pairs of rainfall and Tmax gridded products, the one that showed high agreement with gauge stations was selected as input for trend analysis.

2) Mapping Variability of Climatic Variables

A modified Mann–Kendall statistic [35] was used to test the significance ($p < 0.1$) of monotonic trends for each of the input variable. A modified Mann–Kendall statistic was selected to cater for serial autocorrelation in the monthly time series data. The magnitude of the trend was quantified using the Theil-Sen's median slope estimator [36]. Trend analysis was accomplished using the "eco.theilsen-2" function of "EcoGenetics" R package [37]. For every monthly time-series data, this function produced two grid rasters' representing the p-values from Mann–Kendall significant test and the Theil-Sen's slope estimator. Theil-Sen's slope for areas with $p < 0.1$ were regarded as significant whereas areas with $p < 0.1$ were considered as nonsignificant. Theil-Sen's slope for the three variables was presented in maps using

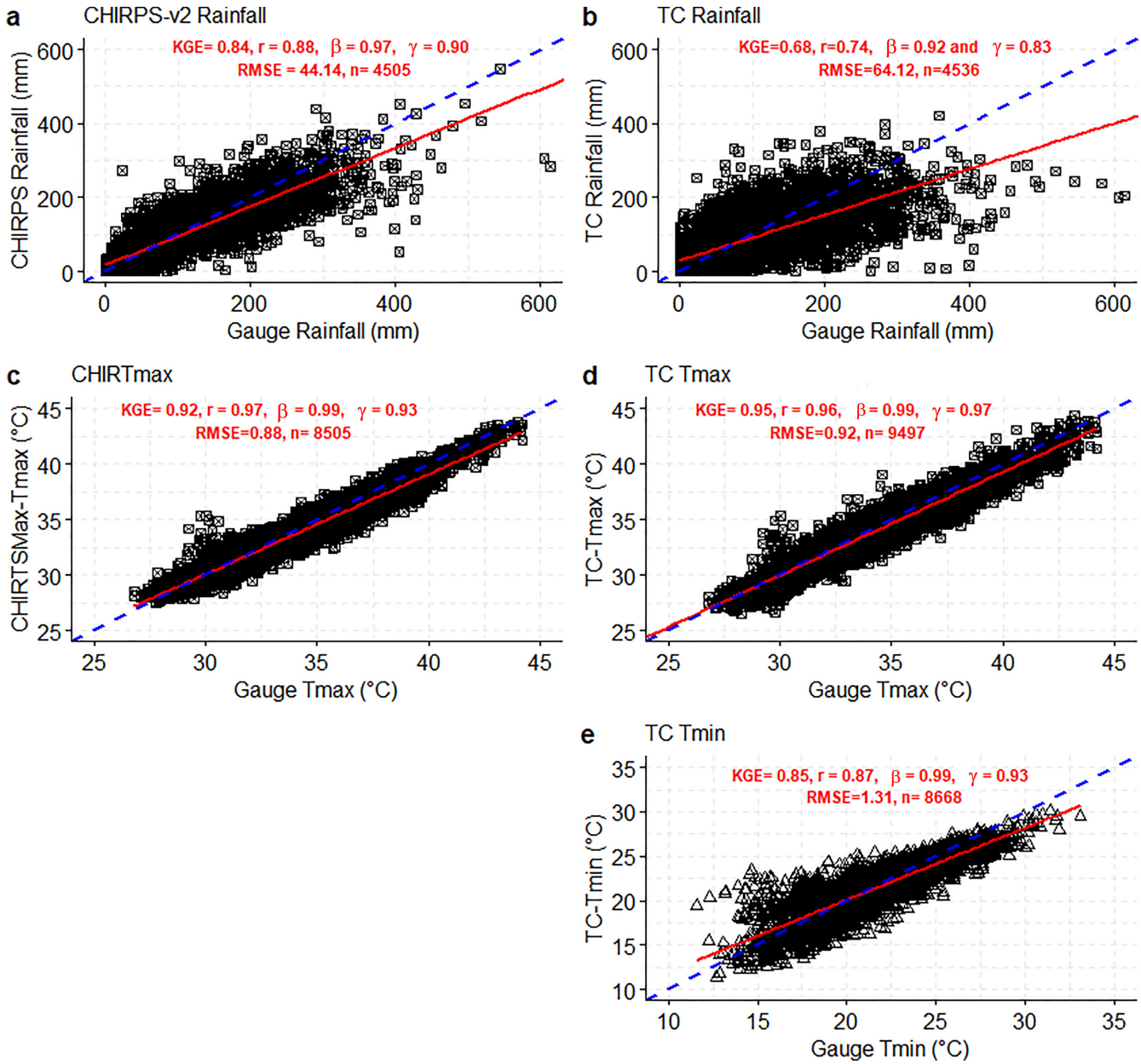

Fig. 3. Comparison between gauge station observations with (a) gridded CHIRPS-v2 rainfall, (b) TC rainfall, (c) CHIRTSmax, (d) TC-Tmax, and (e) minimum temperatures (TC-Tmin) over six countries in West Africa region. The dashed blue line is 1:1 line and the continuous red line is the linear regression line. The units for RMSE are the same as those shown in the *y*-axis.

raster [38] and rasterVis [39] R packages. Areas showing a significant trend ($p < 0.1$) were highlighted on the maps with hatched lines using cartography [40] R package.

Moreover, the differences in climatic trends between the six AEZs in the study area (see Fig. 1) was investigated by comparing the significant monthly Theil-Sen's slope (magnitude of trend) for the three climatic variables. Boxplots were generated to visualize the differences in climatic trends between AEZs for each month. For grid cells where an overlapping significant trend was observed for all the three variables, a correlation analysis was conducted to examine their relationship. The Kendall tau correlation was used to examine the relationship between the trend of rainfall and the two extreme temperature variables at a nominal significance level of $p = 0.05$. A grouping factor was added as input in the correlation analysis to represent a combination of months and AEZs.

III. Results

A. Evaluating Gridded Climatic Variables Against Gauge Data

All gridded monthly climate products except TC-rainfall estimated the gauge station observations with very high accuracy (KGE $\geq$ 0.84; Fig. 3). The gridded CHIRPS-v2 rainfall product showed higher accuracy [KGE $>$ 0.84, Fig. 3(a)] compared to TC-rainfall product [KGE $>$ 0.67, Fig. 3(b)]. For both

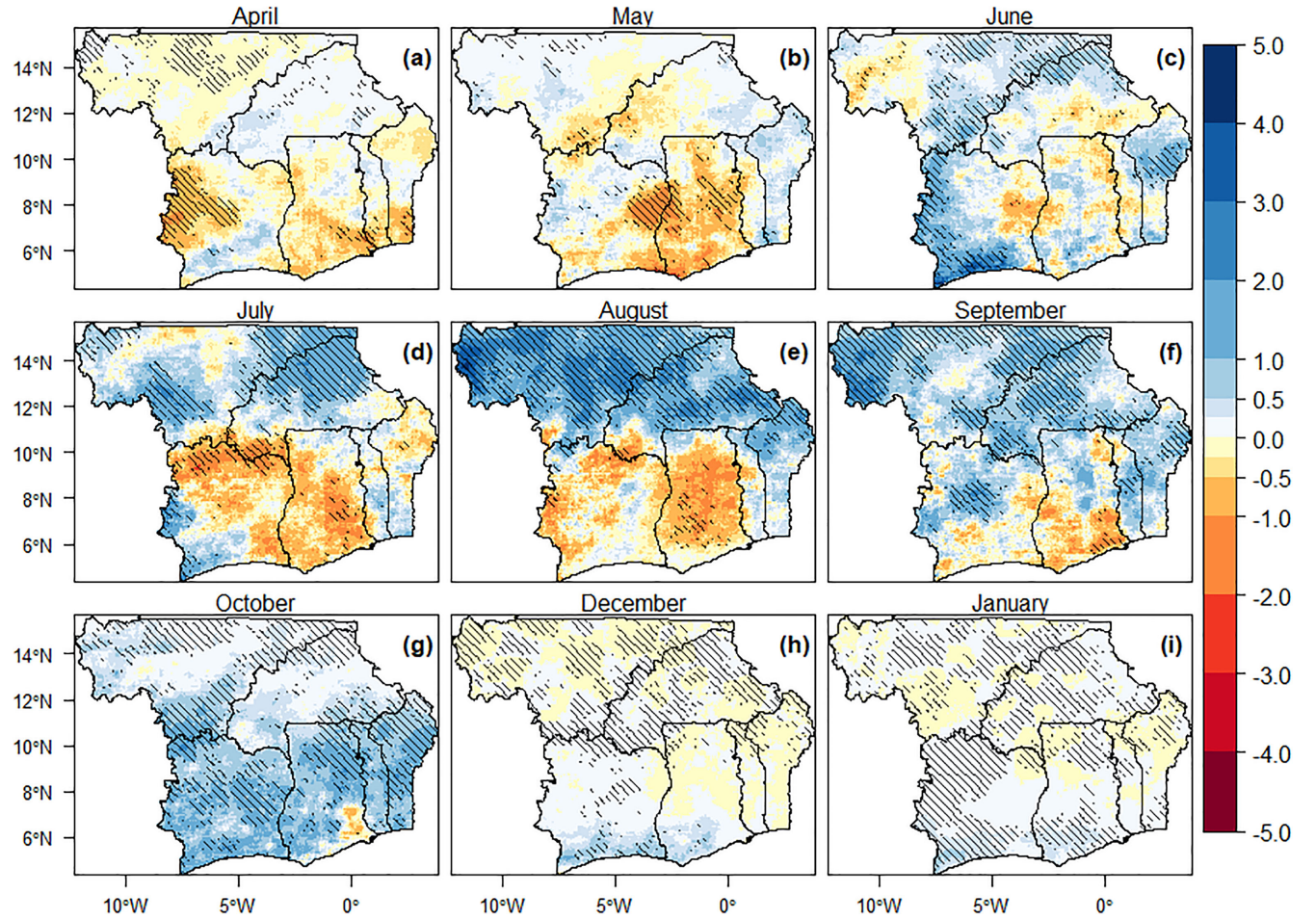

Fig. 4. Spatial–temporal trends of monthly CHIRPS-v2 rainfall (mm/month/year) over six West African countries for 37 years period (1981–2017). The blue and yellow-red tones represent grid cells with positive and negative trends, respectively. The black hachures superimposed over the raster layer shows the area with significant Theil-Sen's slope ($p < 0.1$).

CHIRPS-v2 and TC rainfall products, the underestimation bias of rainfall values above 100 mm was higher and more prevalent compared to the overestimation bias of low values (below 100 mm). However, the TC-rainfall [see Fig. 3(b)) showed higher underestimation bias compared to CHIRPS-v2 data [see Fig. 3(a)]. The gridded CHIRPS-v2 time series was subsequently selected to quantify long-term trends of rainfall (see Section III-B), given its higher accuracy compared to TC rainfall data. The TC Tmax showed slightly higher overall accuracy (KGE = 0.95) compared to CHIRTSmax (KGE = 0.92), therefore, the former was selected as input for trend analysis. The gridded monthly Tmin data showed high agreement with gauge records [KGE > 0.85, Fig. 3(e)], although estimates below 20 °C were more uncertain. This estimation bias reduced with increasing Tmin values.

B. Spatial–Temporal Trends of Climatic Variables

CHIRPS-v2 rainfall showed a significant ($p < 0.1$) positive trend ranging from 0.1 to 5 mm/month/year from June to October with a peak in August [see Fig. 4(c)–(g)] but with varying spatial distribution over West Africa. The positive trend of June to September rainfall mainly occurred north of 11° latitude within the AEZs 2, 3, and, 4 [Sahel, Sudan, and northern Guinea savanna; Fig. 4(c)–(f)]. In contrast, rainfall in October showed a significant ($p < 0.1$) positive trend (0.1–3 mm/month/year) over 75% of the region, but the magnitude of increase was higher in the region South of 11° latitude [see Fig. 4(g)]. April rainfall showed a significant decline (−0.1 to −2 mm/month/year) over western Ivory Coast and Southern Mali. A significant decline of May rainfall occurred along the trans-boundary region between Ivory Coast and Ghana and in the Volta Basin in west-central Ghana. December and January rainfall showed significant ($p < 0.1$) negative and positive trends but of low magnitude (<1 mm/month/year), although the positive trend covered a larger area. Rainfall trends for dry season months (November, February, and March) were not calculated since these time series were characterized by deficient rainfall and with many data gaps.

TC Tmax and Tmin variables showed significantly ($p < 0.1$) warming trends (0.005–0.067 °C/month/year) in all months but with different spatial distribution across the region (see Figs. 5 and 6). However, a localized significant ($p < 0.1$) cooling was observed between August [see Fig. 5(e)–(g)] and September

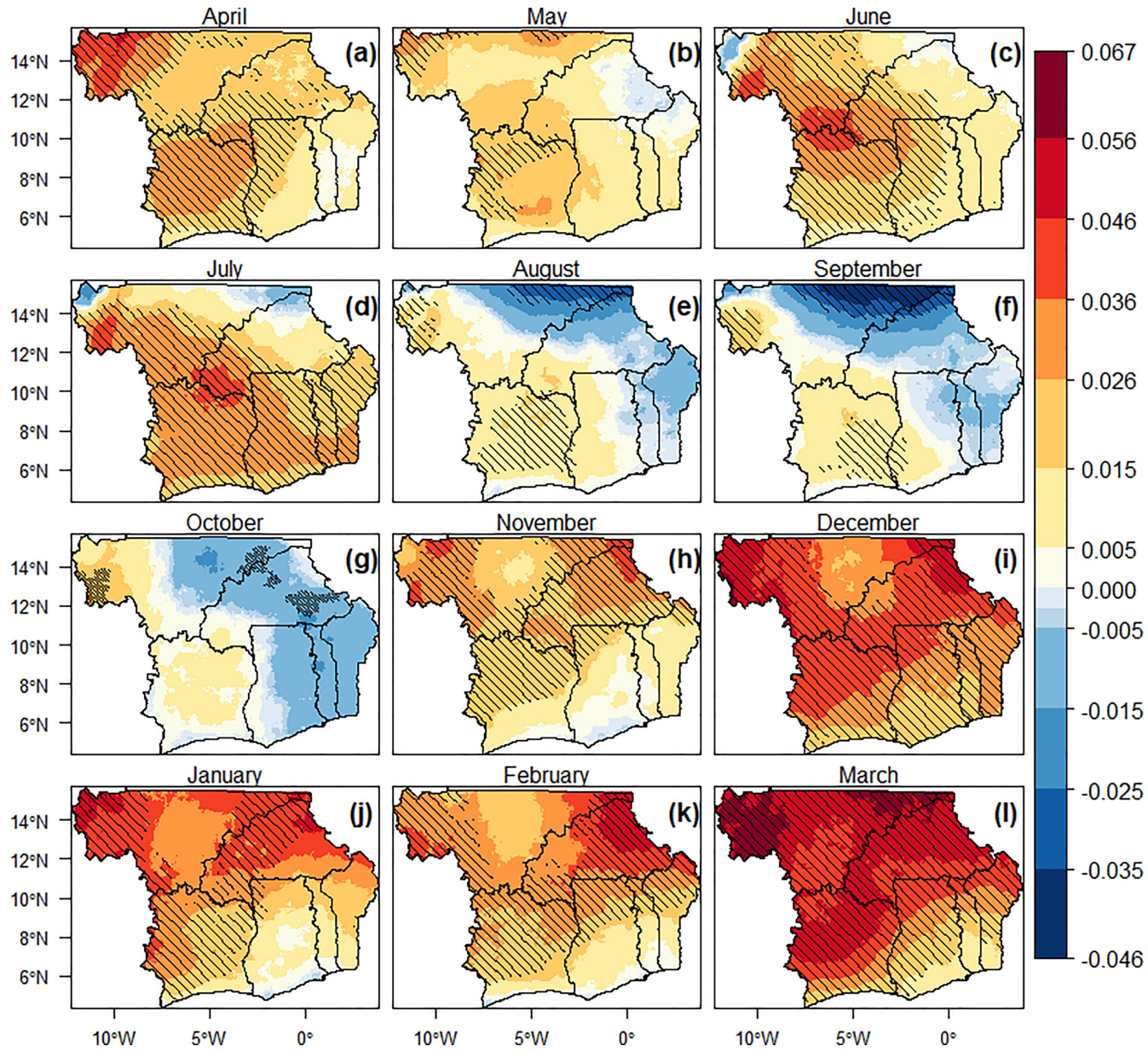

Fig. 5. Spatial-temporal trend of monthly TC-Tmax (°C/month/year) over six West African countries for 37 years period (1981–2017). The blue and yellow-red tones represent areas with cooling and warming trends, respectively. The black hachures superimposed over the raster layer show the area with significant Theil-Sen's slope ($p < 0.1$).

[Fig. 6(e)–(g)] in Southern Mali and Northern Burkina Faso, an area that also experienced a significant increase in rainfall in the same period [see Fig. 4(e)–(f)]. The range of change of Tmin was narrower (−0.033 to 0.047 °C/month/year) compared to Tmax (−0.045 to 0.067 °C/month/year). The TC Tmax during October was mostly insignificant [see Fig. 5(g)], but Tmin showed significant warming in over 50% of the region [see Fig. 6(g)]. The most severe and widespread warming trend of Tmax was recorded in March compared to October and November for Tmin.

C. Magnitude of Climatic Trends Between AEZs

Zonal analysis of the magnitude of significant trends of the three monthly climatic variables revealed varied patterns across the six AEZs. CHIRPS-v2 rainfall for April showed a negative trend in AEZs 6 and 7 [median = −0.74 mm/month/year, Fig. 7(a)], while the rest of AEZs had a marginal trend. May rainfall showed a marginally significant increase in AEZ 2 and 3 (0.14–0.28 mm/month/year) but declined in all the other AEZs [−0.42 to −1.18 mm/month/year, Fig. 7(b)]. June, September, and October rainfall showed a positive trend in all AEZs (median = 0.19–1.83 mm/month/year), and the magnitude of the trend increased in a consistent pattern moving from AEZ 2 to 7 [see Fig. 7(c), (f), and (g); Appendix B). July rainfall showed a negative trend in AEZs 5 and 6 but increased in all the other zones. August rainfall had a positive trend in all AEZs (median = 1.06–2.01 mm/month/year) except a decline in AEZ 7 (median = −0.95 mm/month/year). December and

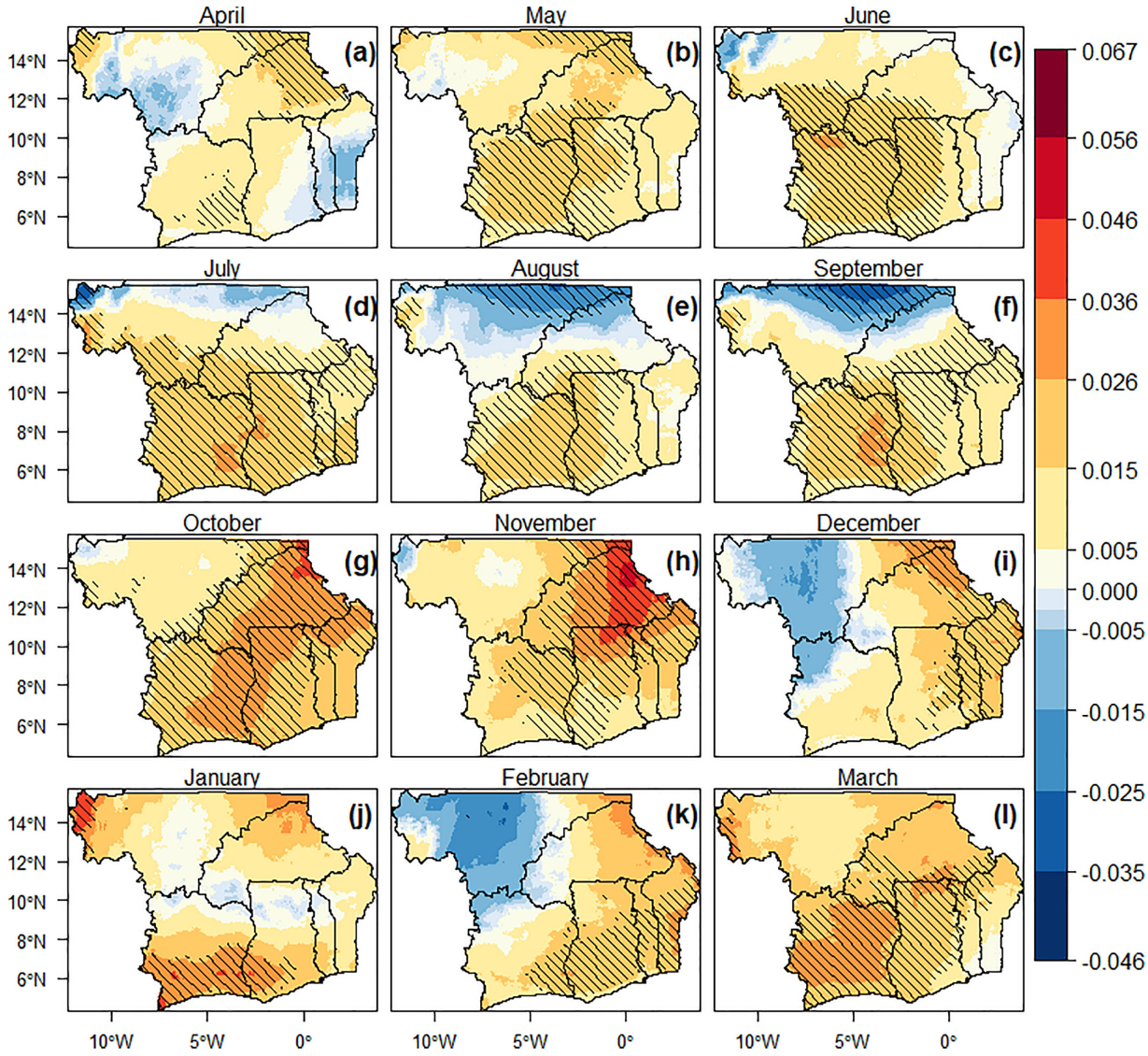

Fig. 6. Spatial–temporal trends of monthly TC minimum temperature (Tmin) expressed in °C/month/year over six West African countries for 37 years period (1981–2017). The blue and yellow–red tones represent areas with cooling and warming trends, respectively. The black hachures superimposed over the raster layer show the area with significant Theil-Sen's slope ($p < 0.1$).

January rainfall showed a remarkable positive trend only in AEZ 7 (0.23–0.64 mm/month/year).

Tmax and Tmin showed consistent warming trend across all AEZs and months except July–October when a significant cooling was observed in one or both parameters in AEZ 2 and 3 (see Figs. 8 and 9). The positive trend of Tmax and Tmin from November to May was in most instances highest at AEZ 2 and lowest at AEZ 7 [see Figs. 8(b)–(h) and 9(b)–(h)]. The highest positive trend of Tmax was observed during March at AEZ 2 (0.055 °C/month/year), followed by AEZ 3 (0.051 °C/month/year). The observed cooling trend for both Tmax [see Fig. 7(e) and (f)] and Tmin [see Fig. 8(e) and (f)] from August to September in AEZs 2 and 3 coincided with a positive trend of rainfall [see Fig. 7(e) and (f)].

Results revealed a significant negative correlation ($r = -0.21$, $p < 2.2e{-}16$) between trends of rainfall and Tmin at AEZ2 during August [see Fig. 10(a)]. Trends of rainfall and the two extreme temperature variables at all the other combinations of AEZs and months showed a significant positive correlation [$r =$ 0.15 to 0.62, $p < 5e{-}7$, Fig. 10(b)].

IV. Discussions

In West Africa, CHIRPS-v2 satellite-based rainfall was more accurate than TC reanalysis product, although the TC data has a finer spatial resolution (4 km) compared to CHIRPS-v2 (5.5 km). In contrast, the reanalysis TC Tmax gridded data showed slightly higher agreement with gauge data compared to the satellite multidata source (CHIRTSmax) product. Moreover, the gridded temperature variables [see Fig. 3(c)–(e)] showed a higher correlation with gauge station data compared to the two gridded rainfall products [see Fig. 3(a) and (b)]. Other interpolated

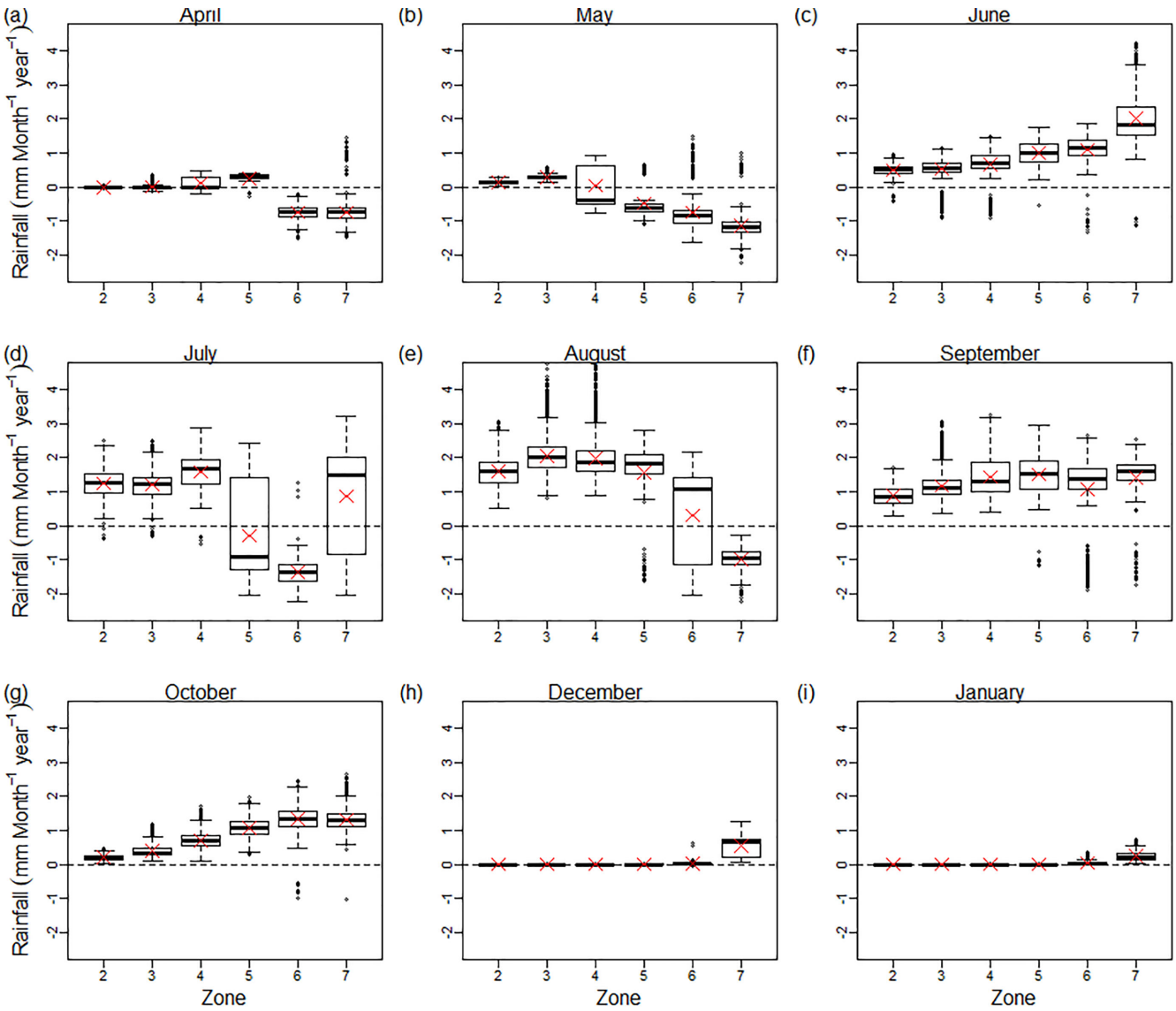

Fig. 7. Variability of trends of monthly CHIRPS-v2 rainfall over six AEZs in West Africa. Only values from grid cells that showed a significant trend ($p < 0.1$) in Fig. 4 are shown. The X sign in the boxplot indicates the mean of the trend. The spatial extent of AEZs is shown in Fig. 1

climatic surfaces such as WorldClim-2 [25] reported a lower accuracy of rainfall compared to temperature variables. Rainfall exhibits high spatial and temporal variability, such as the abrupt changes along the rain shadows. In contrast, temperature exhibits a rather smooth latitudinal and altitudinal gradient. Even when disrupted, for example, by coastal effects, the resulting changes are rather gradual [25].

Recent evaluations of monthly gridded CHIRPS-v2 data against gauge station observations in West Africa reported a high correlation that is similar to the results reported in this study [15], [18], [28]. The higher accuracy of CHIRPS- v2 data is because the product was generated from high-resolution climatology, multiple satellite products, and the algorithm incorporated a bias correction using the gauge station data [12]. The higher bias observed in TC rainfall data could emanate from the fact that the product was produced through downscaling of coarser resolution (0.5°) CRU grids that are generated by interpolation of spatially skewed gauge stations data [26]. The low density of gauge observations used to estimate the original CRU product could have resulted in poor representation of local rainfall processes that are predominantly convective [41]. The lower accuracy of TC rainfall in West Africa compared to CHIRPS-v2 echoes earlier findings by [20] that the performance of gridded rainfall products exhibit differences from region to region and is also dependent on the timescale of observation, season, and topography. Comparing accuracy between relatively new gridded datasets such as CHIRPS-v2, CHIRTSmax, and TC rainfall is recommended to ascertain which ones are more reliable at particular locations or context. However, to the best of the author's knowledge, this study is the first attempt to validate TC monthly time series dataset in Africa.

The evaluation of gridded climate products was not completely independent because a proportion of gauge stations data is input to the satellite-based algorithms; either directly for

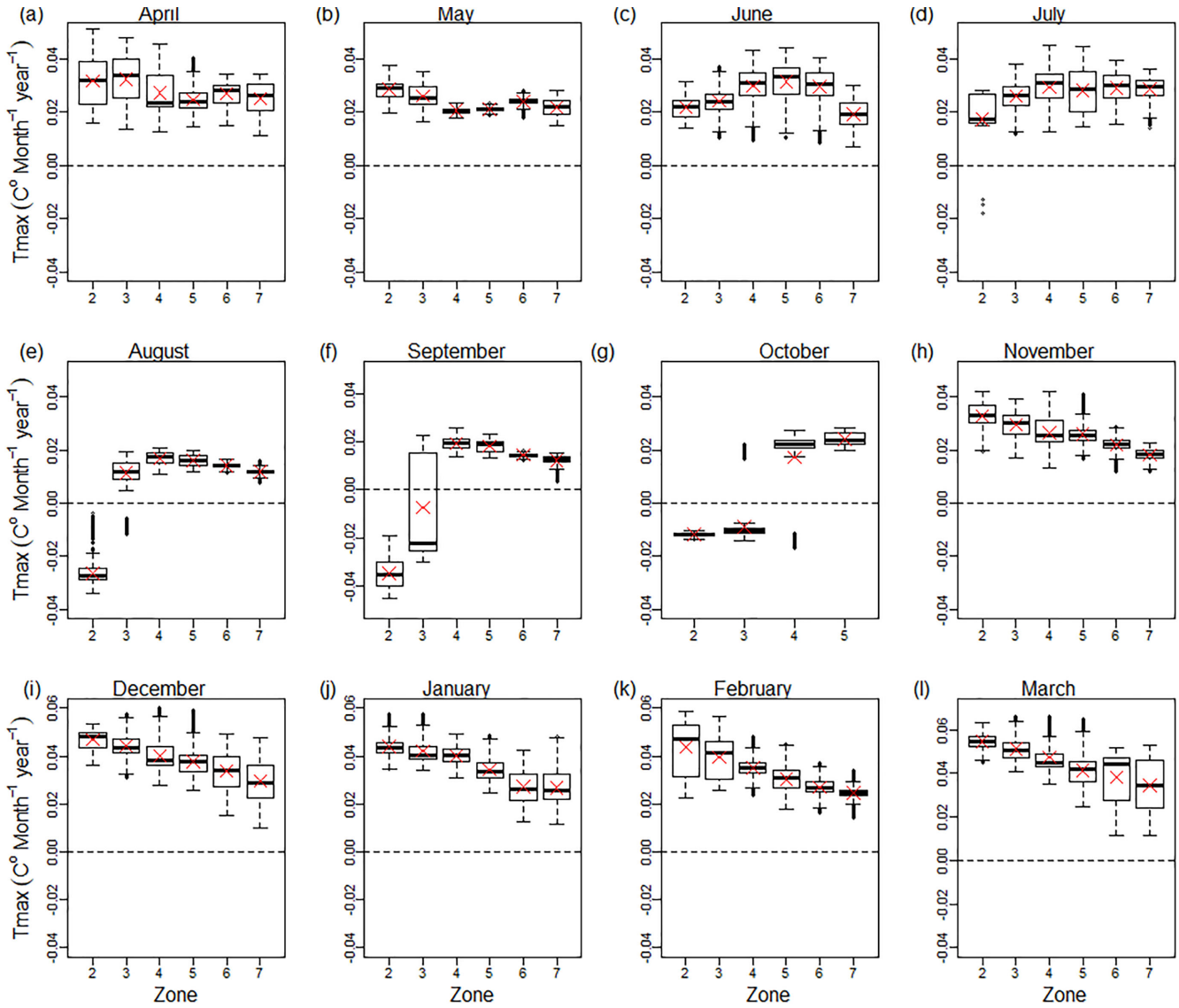

Fig. 8. Variability of trends of TC maximum temperatures (Tmax) over six AEZs in West Africa. Only values from grid cells that showed a significant trend ($p < 0.1$) in Fig. 5 are shown. The X sign in the boxplot indicates the mean of the trend. The spatial extent of AEZs is shown in Fig. 1.

CHIRPS-v2 [12] and CHIRTSmax [13] or indirectly for TC data [14]. The TC data was originally derived from the CRU Ts4.0 and WorldClim climatologies that were interpolated from a fraction of gauge stations data [14]. Some of the gridded products such as CHIRPS-v2 use a different number of stations over the years due to the prevalent decline of gauge stations data [12]. This situation further complicates the identification of a completely independent set of gauge stations

A point to pixel procedure was utilized to assess the accuracy of the gridded climate variables. A mismatch between the scale of two datasets can introduce bias during accuracy assessment [14]. There is a potential risk of scale-dependent bias in the current evaluation because the values of climate variables at the location of a gauge station were compared with values of the corresponding grid cell that covered approximately four-square kilometers. However, the severity of such bias is more critical in regions with complex terrain where the altitude of a station may differ substantially from the average elevation of a colocated grid cell. However, this should not be a significant source of error in West Africa, where topographical gradients are mainly gradual.

CHIRPS-v2 rainfall showed significant ($p < 0.1$) increasing trend (0.1–3mm/month/year) along the Sahel, Sudan, and northern Guinea savanna zones (AEZ 2, 3, and 4) [see Fig. 4(c)–(f) and Fig. 7(c)–(f)], from June to September with peak increase recorded in August, which is the wettest month in above AEZs. Sanogo *et al.* [17] observed a positive trend of rainfall along the West Africa Sahel that peaked in August. The significant positive trend of rainfall over AEZ 2 and 3 during the wet season peak in August and September was combined by significant cooling [see Figs. 7–9]. Increased rainfall amplified the Tmin cooling effect at AEZ2 in August. The inverse correlation between the positive rainfall trend and the cooling of day and nighttime temperatures is well documented in west Africa. Oueslati *et al.* [42] reported

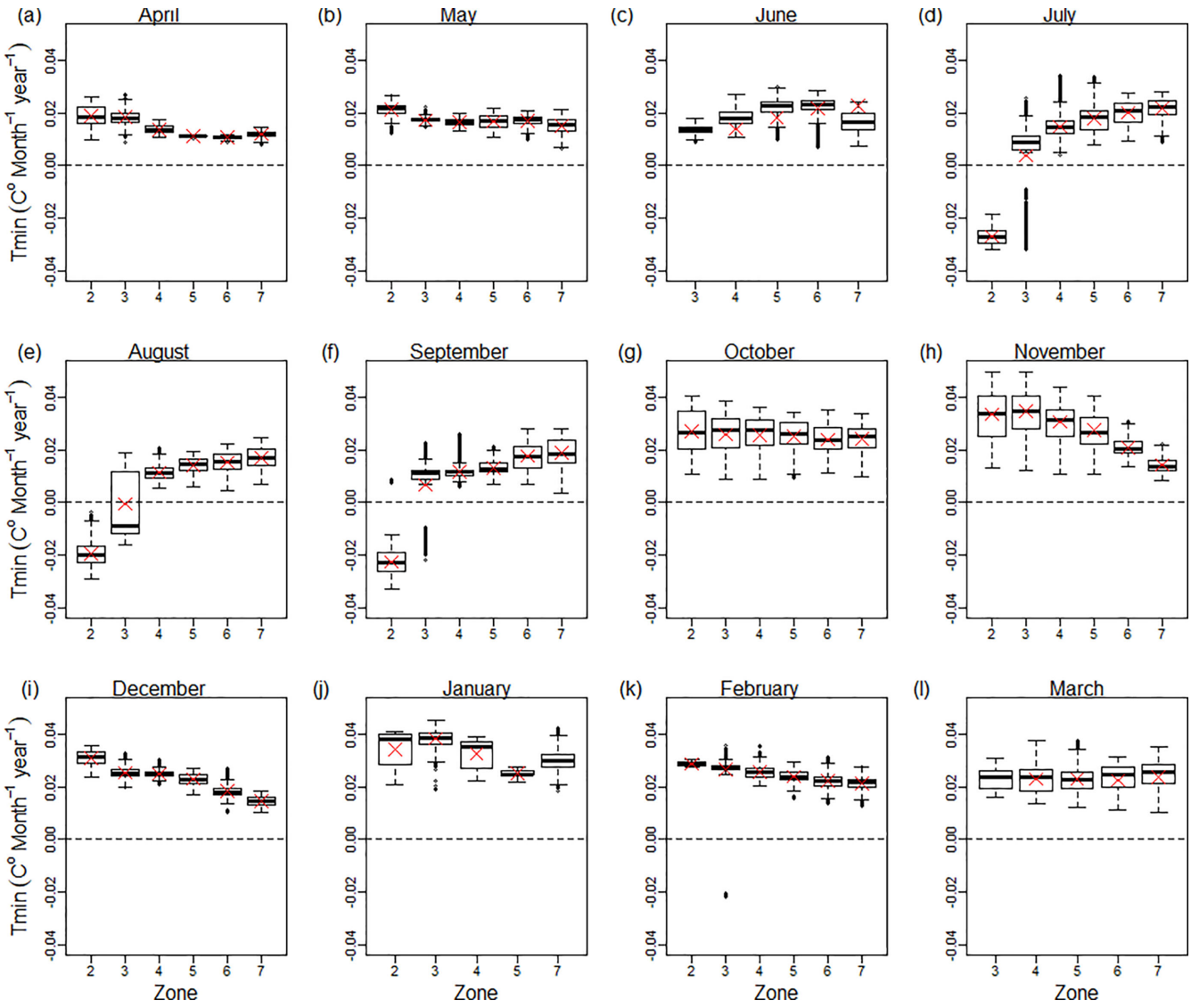

Fig. 9. Variability of trends of TC minimum temperature (Tmin) over six AEZs in West Africa. Only values from grid cells that showed a significant trend ($p < 0.1$) in Fig. 6 are displayed. The X sign in the boxplot indicates the mean of the trend. The spatial extent of AEZs is shown in Fig. 1.

a sharp drop in surface temperatures after rainfall events in Burkina Faso. This is partly because of the convective activities that increase the daytime cloud cover that, in-turn, attenuates the incoming solar radiation. A recent long-term (1854–2014) evaluation of rainfall trends using 602-gauge records over a larger area in West Africa, reported a substantial recovery of August–October rainfall [11]. However, the evaluation suggested that rain has not fully recovered to the era of persistent wet conditions that prevailed before 1968 across the region. Therefore, the significant positive trends observed in this article could be part of a transition state toward the wetter conditions.

Recent studies have associated the greening trend along the Sahel belt of West Africa to the prevalent increase of growing season rainfall [43], [41]. Usman *et al*. [28] reported a positive trend of CHIRPS-v2 rainfall between August and October, with a peak of 4 mm/year in August, over the Sudan-Sahelian savanna in Nigeria, northern Togo, and western Burkina Faso. This change was observed for a period of 35 years (1981–2015). They observed that the positive trend of rainfall coincides with the late maturity of sorghum and millet, which are the main staple cereal crops in this zone. The significant increase in rainfall during the late growing season over the Sudano-Sahelian savanna in Nigeria is especially crucial for sorghum and millet production since late drought impedes swelling of the grain, thus affecting dry weight production. Drought before the flowering stage of millet could reduce yields by over 70%. Sorghum is particularly sensitive to late-season rainfall as the crop does not enter the high water use period during its life cycle until August. The positive trend of rainfall during the peak of the growing season reduces the risk of detrimental drought during the ripening stage of sorghum.

There is a growing body of evidence that farmers are adapting to increased rainfall in Sahel and Sudan-savanna in West Africa. For example, Lalou *et al*. [4] observed that an increase in total

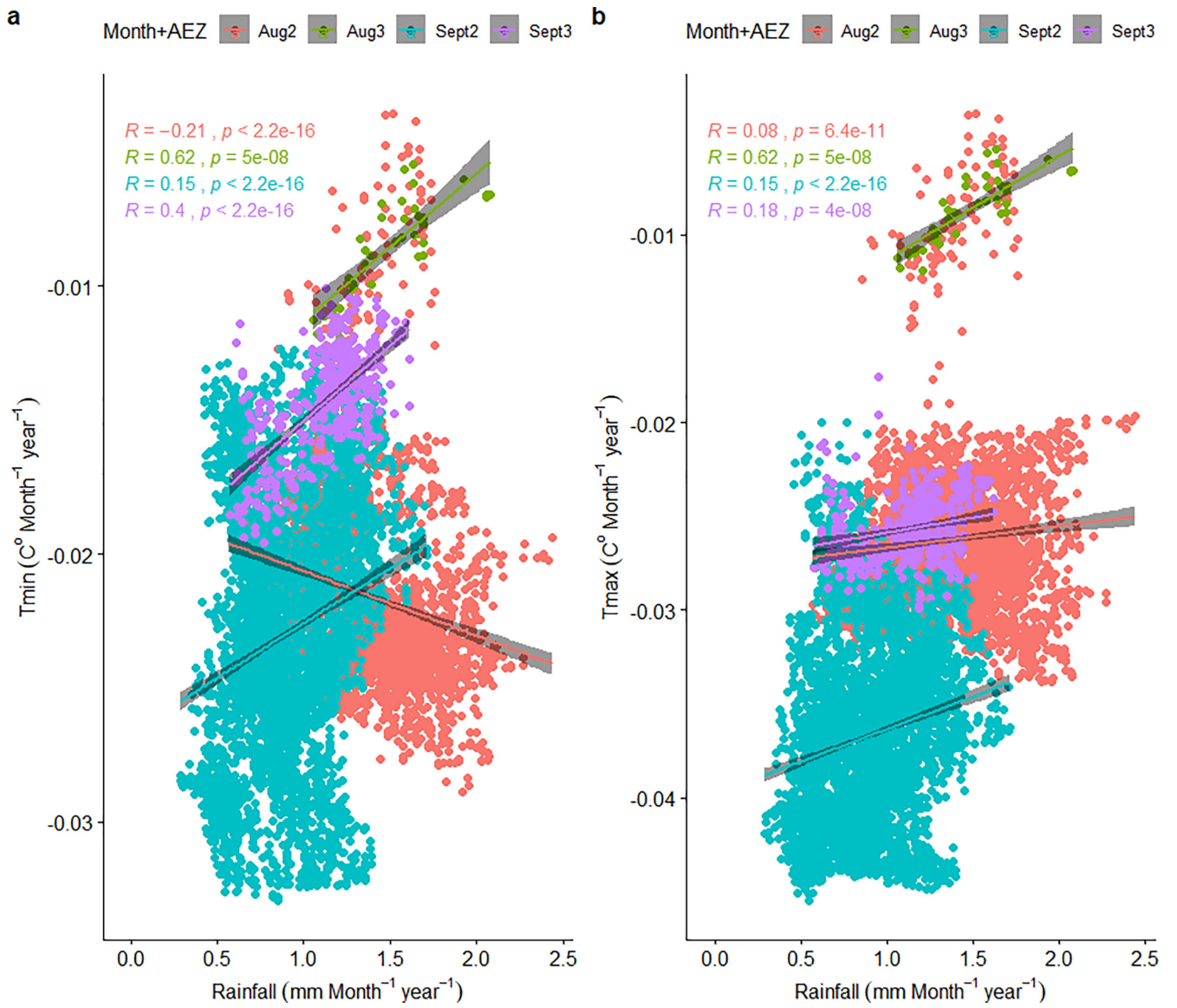

Fig. 10. Correlation between trends of CHIRPS-v2rainfall versus TC Tmin (a) and CHIRTSMax Tmax (b) for Sahel (AEZ-2) and Sudan Savanna (AEZ-3) of West Africa during August and September. Only values from grid cells showing overlapping significant trends ($p < 0.05$) for the three variables in Figs. 4–6 are included in the correlation analysis. The linear regression lines are shown with 95% confidence interval is shaded in gray color.

annual rainfall improved the adoption of Sanio pearl millet variety along a North–South gradient in the Sahel over Senegal. Sanio pearl millet variety requires more water and takes longer to mature compared to the dominant Souna millet that ripens early (80 days) and better adapted to droughts. They observed that an average of 6.3 new villages adopted Sanio millet per year when the average rainfall during the growing season was 415 mm. However, adoption exceeded 25.6 villages per year when average rainfall was between 580 and 620 mm. Results from this study provide further evidence on priority locations for scaling out appropriate agronomic and animal husbandry technologies to take advantage of the improved agricultural potential in the Sahel and Sudan-Savanna agroecologies.

However, the observed positive trend of rainfall during the wettest months, over the three arid-to-semiarid agroecologies, can counter-intuitively accentuate floods and waterlogging. Floods are frequent in the study area [44]. Moreover, increased late-season rainfall (September–October) over AEZ 2–3 reportedly caused rotting of mature millet and groundnuts crops, thereby increasing preharvest losses [44]. Therefore, appropriate adaptive measures are required to harness the increased moisture and control its adverse effects on croplands and rangelands at AEZ 2–3. The positive but low-magnitude rainfall trend recorded during the dry months (January–December) at the humid forest zone (AEZ-7) can offer dry season pastures. However, the rainfall trends observed during these arid months should be treated with caution, considering that CHIRPS-v2 product showed a tendency to overestimate low-magnitude rainfall events. The significant positive rainfall trends observed from June to October along most AEZs could also be underestimated.

Warming trends dominated in most agroecologies, except for a few instances of localized cooling during August and September over AEZ2 and AEZ3. Aguilar *et al*. [45] observed a similar warming trend in Guinea that was characterized by hot extremes and fewer cold extremes. A positive trend of rainfall occurred over most AEZs between June and October (see Fig. 7). However, this positive trend largely coincided with significant warming trends. Increased warming can enhance the evaporative loss of soil moisture, thereby attenuating the potential beneficial effect of increased rainfall. The widespread warming trends will directly affect the water balance in West Africa, especially the evapotranspiration component.

Recent studies have quantified the effect of climate change on crop yields [1]–[3]. Zhao *et al*. [3] demonstrated that each degree Celsius increase of global mean temperature reduces global yields of maize, wheat, and rice by 7.4%, 6%, and 3.2%, respectively, though there are considerable variations across space. Ray *et al*. [1] estimated that 1%–45% of the variability in maize yield in different sections of the study area was due to climate variability. In Southern Mali, Traore *et al*. [46] reported that an increase of Tmax by 0.08 °C /year and 1 dry day/year during the rainy season resulted in a yield loss of cotton equivalent to 24 kg/haand 41 kg/ha, respectively. It would be informative to quantify how the observed warming trends, especially North of 11° latitude where rainfall is increasing or stable, could affect yields of major staple crops. However, the current analysis did not quantify trends of crop yields due to scarcity of matching time series yield data. The next logical step to advance the information generated by this study is to quantify the impact of observed significant changes in climatic variables on crop yields vis-à-vis the current edaphic and agronomic management practices. Undertaking such a study will decipher the magnitude of climatic control over past agricultural production and how the scenario can unfold in the future if the observed climatic trends prevail or escalate. Time series data for crop yields at farm level would support the calibration of robust models for estimating crop yields using increasingly available remote sensing data. Initiatives that promote efficient record-keeping at the farm level and increasing accessibility of such data for research are a priority.

V. Conclusion

CHIRPS-v2 rainfall, CHIRTSmax, TC-Tmax, and TC-Tmin accurately estimated gauge station data. Therefore, these gridded datasets can reliably complement the sparse gauge station network in West Africa. Increased availability of freely available gridded data facilitates a better understanding of spatial–temporal trends of climate to inform the design of evidence-based measures for adapting to climate change and variability. A positive trend of rainfall was observed during the wet season peak from August to September, mainly North of 11° latitude. A widespread significant warming trend was observed over West Africa in all months that emphasize the need for increased investments of measures to deal with the effects of heat stress on crops. The information generated in this study supports the design of early warning systems against drought and floods.

Supplementary material 1: Characteristics of gauge stations used for accuracy assessment.

Supplementary material 2: Variability of significant trends of Tmax, Tmin, and Tmax for different AEZs and months.

Acknowledgment

The author expresses sincere gratitude to L. Roser for help in the modification of eco.theilsen function used to calculate the climatic trends.

References

[1] D. K. Ray, J. S. Gerber, G. K. Macdonald, and P. C. West, "Climate variation explains a third of global crop yield variability," *Nature Commun.*, vol. 6, pp. 5989–5989, 2015.

[2] K. A. Amouzou *et al.*, "Climate change impact on water- and nitrogen-use efficiencies and yields of maize and sorghum in the northern Benin dry savanna, West Africa," *Field Crops Res.*, vol. 235, pp. 104–117, 2019.

[3] C. Zhao *et al.*, "Temperature increase reduces global yields of major crops in four independent estimates," *Proc. Nat. Acad. Sci.*, vol. 114, pp. 9326–9326, 2017.

[4] R. Lalou, B. Sultan, B. Muller, and A. Ndonky, "Does climate opportunity facilitate smallholder farmers adaptive capacity in the Sahel?" *Palgrave Commun.*, vol. 5, pp. 2019–2019, 2019.

[5] I. Niang *et al.*, *Ar5 Climate Change 2014: Impacts, Adaptation, and Vulnerability. Part B: Regional Aspects. Contribution of Working Group II to the Fifth Assessment Report of the Intergovernmental Panel on Climate Change*. Cambridge, U. K.: Cambridge Univ. Press, 2014, pp. 1199–1265.

[6] J. M. Collins, "Temperature variability over Africa," *J. Climate*, vol. 24, pp. 3649–3666, 2011.

[7] T. Dinku *et al.*, "Validation of the CHIRPS satellite rainfall estimates over eastern of Africa," *Quarter. J. Roy. Meteorol. Soc.*, vol. 144, pp. 292–312, 2018.

[8] S. Contractor *et al.*, "Rainfall estimates on a gridded network (REGEN)—A global land-based gridded dataset of daily precipitation from 1950-2013," *Hydrol. Earth Syst. Sci. Discuss*, vol. 2019, pp. 1–30, 2019.

[9] R. Washington *et al.*, "African climate change: Taking the shorter route," *Bull. Amer. Meteorol. Soc.*, vol. 87, no. 10, pp. 1355–1366, 2006.

[10] K. Owusu and P. R. Waylen, "The changing rainy season climatology of mid-Ghana," *Theor. Appl. Climatol.*, vol. 112, pp. 419–430, 2013.

[11] S. E. Nicholson, A. H. Fink, and C. Funk, "Assessing recovery and change in West Africa's rainfall regime from a 161-year record," *Int. J. Climatol.*, vol. 38, no. 10, pp. 3770–3786, 2018.

[12] C. Funk *et al.*, "The climate hazards infrared precipitation with stations—A new environmental record for monitoring extremes," *Sci. Data*, vol. 2, no. 1, pp. 150 066–150 066, 2015.

[13] C. Funk, P. Peterson, S. Peterson, S. Shukla, F. Davenport, and J. Michaelsen, "A high-resolution 1983–2016 Tmax climate data record based on infrared temperatures and stations by the climate hazard center," *J. Climate*, vol. 32, pp. 5639–5658, 2019.

[14] J. T. Abatzoglou, S. Z. Dobrowski, S. A. Parks, and K. C. Hegewisch, "TerraClimate, a high-resolution global dataset of monthly climate and climatic water balance from 1958–2015," *Sci. Data*, vol. 5, pp. 170 191–170 191, 2018.

[15] I. Larbi, C. F. Hountondji, T. Annor, A. W. Agyare, G. Mwangi, and J. Amuzu, "Spatio-temporal trend analysis of rainfall and temperature extremes in the vea catchment," *Climate*, vol. 6, pp. 2–17, 2018.

[16] M. Baidu, L. K. Amekudzi, N. J. Aryee, and T. Annor, "Assessment of long-term spatio-temporal rainfall variability over Ghana using wavelet analysis," *Climate*, vol. 5, pp. 2–24, 2017.

[17] S. Sanogo *et al.*, "Spatio-temporal characteristics of the recent rainfall recovery in West Africa," *Int. J. Climatol.*, vol. 35, pp. 4589–4605, 2015.

[18] M. Dembele and S. J. Zwart, "Evaluation and comparison of satellite-based rainfall products in Burkina Faso, West Africa," *Int. J. Remote Sens.*, vol. 37, pp. 3995–4014, 2016.

[19] P. Camberlin, G. Barraud, S. Bigot, O. Dewitte, F. Imwangana, and J. C. M. Mateso, "Evaluation of remotely sensed rainfall products over Central Africa," *Quart. J. Roy. Meteorol. Soc.*, vol. 145, pp. 2115–2138, 2019.

[20] C. Tote, D. Patricio, H. Boogaard, R. V. D. Wijngaart, E. Tarnavsky, and C. Funk, "Evaluation of satellite rainfall estimates for drought and flood monitoring in Mozambique," *Remote Sens.*, vol. 7, pp. 1758–1758, 2015.

[21] W. M. Kimani, C. B. J. Hoedjes, and Z. Su, "An assessment of satellite-derived rainfall products relative to ground observations over east Africa," *Remote Sens.*, vol. 9, 2017, Art. no. 430.
[22] C. Funk, J. Michaelsen, and M. Marshall, "Mapping recent decadal climate variations in precipitation and temperature across eastern Africa and the Sahel," in *Remote Sensing of Drought: Innovative Monitoring Approaches*, B. D. Wardlow, M. Anderson, and J. Verdin, Eds. Boca Raton, FL, USA: CRC Press, 2012, pp. 331–358.
[23] S. E. Nicholson *et al.*, "Temperature variability over Africa during the last 2000 years," *Holocene*, vol. 23, pp. 1085–1094, 2013.
[24] K. Owusu, "Rainfall changes in the savannah zone of northern Ghana," *Weather*, vol. 73, pp. 46–50, 1961.
[25] S. E. Fick and R. J. Hijmans, "WorldClim 2: New 1-km spatial resolution climate surfaces for global land areas," *Int. J. Climatol.*, vol. 37, pp. 4302–4315, 2017.
[26] I. Harris, P. D. Jones, T. J. Osborn, and D. H. Lister, "Updated high-resolution grids of monthly climatic observations—The CRU TS3.10 dataset," *Int. J. Climatol.*, vol. 34, pp. 623–642, 2014.
[27] S. Kobayashi *et al.*, "The JRA-55 reanalysis: General specifications and basic characteristics," *J. Meteorol. Soc. Japan. II*, vol. 93, pp. 5–48, 2015.
[28] M. Usman, J. E. Nichol, A. T. Ibrahim, and L. F. Buba, "A spatio-temporal analysis of trends in rainfall from long term satellite rainfall products in the Sudano Sahelian zone of Nigeria," *Agricultural Forest Meteorol.*, vol. 260–261, pp. 273–286, 2018.
[29] J. H. Lawrimore, R. Ray, S. Applequist, B. Korzeniewski, and M. J. Menne, Global summary of the month (GSOM), Version 1, Nat. Centers Environ. Inf., Boulder, CO, USA, 2016.
[30] M. J. Menne, I. Durre, R. S. Vose, B. E. Gleason, and T. G. Houston, "An overview of the global historical climatology network-daily database," *J. Atmos. Ocean. Technol.*, vol. 29, pp. 897–910, 2012.
[31] S. S. Jagtap, "Environmental characterization of the moist lowland Savanna of Africa," in *Proc. Moist Savannas Africa: Potentials Constraints Crop Prod.*, 1995, pp. 9–30.
[32] G. Fischer *et al.*, *Global Agro-Ecological Zones (GAEZ v3.0)- Model Documentation*, 2012. IIAS, Laxenburg, Austria; FAO Rome, Italy.
[33] H. V. Gupta, H. Kling, K. K. Yilmaz, and G. F. Martinez, "Decomposition of the mean squared error and NSE performance criteria: Implications for improving hydrological modelling," *J. Hydrol.*, vol. 377, pp. 80–91, 2009.
[34] M. Zambrano-Bigiarini, "hydroGOF: Goodness-of-fit functions for comparison of simulated and observed hydrological time series," 2018, R package version 0.3-10. [Online]. Available: https://github.com/hzambran/hydroGOF.
[35] K. H. Hamed and A. R. Rao, "A modified Mann-Kendall trend test for autocorrelated data," *J. Hydrol.*, vol. 204, pp. 182–196, 1998.
[36] P. Sen, "Estimates of the regression coefficient based on Kendall's tau," *J. Amer. Statist. Assoc.*, vol. 63, pp. 1379–1389, 1968.
[37] L. G. Roser, L. I. Ferreyra, B. O. Saidman, and J. C. Vilardi, "Eco-Genetics: An R package for the management and exploratory analysis of spatial data in landscape genetics," *Mol. Ecol. Resources*, vol. 17, pp. 241–250, 2017.
[38] R. J. Hijmans, "Raster: Geographic data analysis and modeling. R package version 3.0-12," 2020. [Online]. Available: https://CRAN.R-project.org/package=raster.
[39] O. P. Lamigueiro and R. Hijmans, "rasterVis. R package version 0.47," 2019. [Online]. Available: http://oscarperpinan.github.io/rastervis
[40] T. Giraud and N. Lambert, "Cartography: Create and integrate maps in your R workflow," *J. Open Source Softw.*, vol. 1, no. 4, pp. 54–54, 2016.
[41] W. Zhang, M. Brandt, F. Guichard, Q. Tian, and R. Fensholt, "Using long-term daily satellite based rainfall data (1983–2015) to analyze spatio-temporal changes in the Sahelian rainfall regime," *J. Hydrol.*, vol. 550, pp. 427–440, 2017.
[42] B. Oueslati, P. Camberlin, J. Zoungrana, P. Roucou, and S. Diallo, "Variability and trends of wet season temperature in the Sudano-Sahelian zone and relationships with precipitation," *Climate Dyn.*, vol. 50, no. 3–4, pp. 1067–1090, 2018.
[43] A. Bichet and A. Diedhiou, "West African Sahel has become wetter during the last 30 years, but dry spells are shorter and more frequent," *Climate Res.*, vol. 75, pp. 155–162, 2018.
[44] P. Tschakert, R. Sagoe, G. Ofori-Darko, and S. N. Codjoe, "Floods in the Sahel: An analysis of anomalies, memory, and anticipatory learning," *Climatic Change*, vol. 103, pp. 471–502, 2010.
[45] E. Aguilar, A. Barry, M. Brunet, L. Ekang, A. Fernandes, and M. Massoukina, "Changes in temperature and precipitation extremes in western central Africa Guinea Conakry, and Zimbabwe, 1955–2006," *J. Geophys. Res. Atmos.*, vol. 114, pp. 2–11, 1955.
[46] B. Traore, M. Corbeels, M. T. van Wijk, M. C. Rufino, and K. E. Giller, "Effects of climate variability and climate change on crop production in southern Mali," *Eur. J. Agronomy*, vol. 49, pp. 115–125, 2013.

Francis Muthoni received the B.A. degree in geography from Moi University, Eldoret, Kenya, the M.Sc. degree in geo-information and earth observation in environmental modelling and management though the European Erasmus Mundus program offered jointly by University of Twente, Enschede, The Netherlands; University of Southampton, Southampton, UK; Lund University, Lund, Sweden; and the University of Warsaw, Warsaw Poland, and the Ph.D. degree in spatial ecology from the University of Twente, Enschede, The Netherlands.

He is currently an Associate Scientist (GIS Specialist) with the International Institute of Tropical Agriculture, Arusha, Tanzania. His research interest focuses on the spatial targeting of agricultural technologies.